

# Thermal expansion behavior of Cu/Cu<sub>2</sub>O cermets with different Cu structures

W.Z. Shao, L.C. Feng, L. Zhen<sup>\*</sup>, N. Xie

*School of Materials Science and Engineering, Harbin Institute of Technology, Harbin 150001, China*

Received 2 January 2009; received in revised form 16 January 2009; accepted 14 March 2009

Available online 14 April 2009

## Abstract

Cu/Cu<sub>2</sub>O cermets were prepared with Cu<sub>2</sub>O matrix imbedded with branch-like or spherical Cu powders. The coefficients of thermal expansion (CTE) of them were tested. The CTE curves can be divided into three segments. From 25 °C to 150 °C, CTEs were found to decrease with temperatures. The CTEs were influenced by the structure of the conductor phase. For cermets prepared with spherical Cu, the increase in CTEs was basically linear with temperatures above 150 °C. In contrast, cermets with same Cu content prepared with branch-like Cu had a CTE with an increasing rate as the temperature rose from 150 °C to 900 °C, and the increasing rates in these temperature range are much higher than those prepared with spherical Cu.

© 2009 Elsevier Ltd and Techna Group S.r.l. All rights reserved.

**Keywords:** C. Thermal expansion; Cu/Cu<sub>2</sub>O cermet; Different Cu structure

## 1. Introduction

Cermet materials, defined as ceramics combining with metals, are widely investigated and applied in industries recently [1,2]. They combine high thermal conductivity from metals with low thermal expansion from ceramics, thus, they can be used in SOFC [3], as an inert anode for aluminum production [4–6], and in some power chips [7]. The coefficient of thermal expansion (CTE), one of the most important properties of cermets, has been widely studied through both experiments and computer simulations [8–10]. Cu/Cu<sub>2</sub>O cermet is a typical cermet material combining high thermal conductivity metal, Cu, with low thermal expansion ceramic, Cu<sub>2</sub>O. Saito et al. [7] studied thermal conductivity and thermal expansion behavior of Cu/Cu<sub>2</sub>O cermet, and found that CTE of Cu/Cu<sub>2</sub>O cermet is in the range of  $9\text{--}14 \times 10^{-6} \text{ }^{\circ}\text{C}^{-1}$  depending on Cu content.

In other studies, many theories or models were used to predict final CTE of cermets [11]. The rule of mixture, the simplest model to predict the CTE of cermets, is expressed as follows:

$$\alpha_c = \alpha_p f_p + \alpha_m f_m \quad (1)$$

where  $\alpha_c$ ,  $\alpha_p$ , and  $\alpha_m$  are the CTE of the cermet, the second phase, and the matrix, respectively, while,  $f_p$  and  $f_m$  are the volume fraction of the second phase and the matrix, respectively. Schapery's model [12] was also widely used to predict the CTE of cermets. This model can be described as

$$\lambda_L = \frac{E_I \lambda_I f + E_M \lambda_M (1 - f)}{E_I f + E_M (1 - f)} \quad (2)$$

where  $\lambda_L$  is the CTE of the cermet,  $\lambda_I$  and  $\lambda_M$  are the CTEs of the metal phase and the ceramic phase,  $E_I$  and  $E_M$  are the Young's modulus of the metal phase and the ceramic phase. Karadeniz [11] reviewed other models that can predict CTE of fiber reinforced composites. Most of these theories or models, however, have no parameters used to describe the structure factor of the second phase, which is very important to the final properties of cermets.

In order to demonstrate the structure dependence of the second phase in cermet materials, CTE of Cu/Cu<sub>2</sub>O cermets with two types of Cu structures and different Cu contents were studied.

## 2. Experimental

Commercial grade Cu<sub>2</sub>O and Cu powders were supplied by Taixing and Chongqing Powder Co., P.R. China with purity of

<sup>\*</sup> Corresponding author. Tel.: +86 451 86412133; fax: +86 451 86413922.

E-mail address: [lzhen@hit.edu.cn](mailto:lzhen@hit.edu.cn) (L. Zhen).

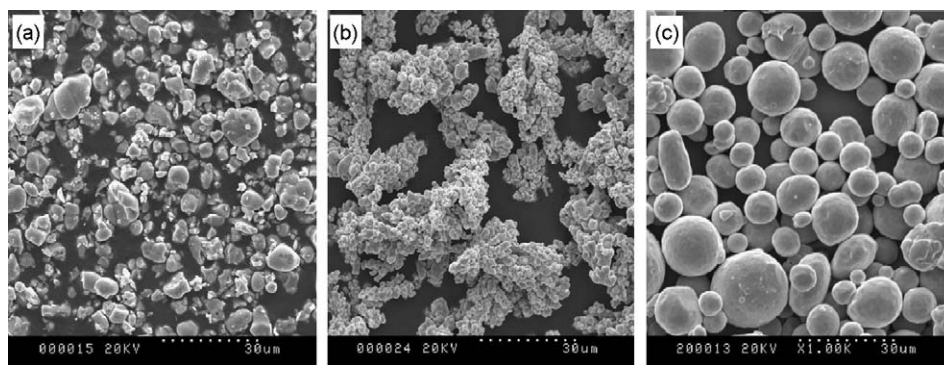


Fig. 1. SEM microstructures of the raw materials: (a)  $\text{Cu}_2\text{O}$  powder, (b) branch-shape Cu powder, and (c) spherical Cu powder.

99.8% and 97%, respectively. In the present study, two types of Cu powders were used for preparing the final cermets. Fig. 1 shows the SEM morphology of  $\text{Cu}_2\text{O}$  and two types of Cu powders. This figure shows that the powder morphology of Cu was either branch-like or spherical, while the shape of the  $\text{Cu}_2\text{O}$  powder was irregular and had unevenly distributed size. To diminish the amount of oxygen on the Cu surface, Cu powders were reduced in  $\text{H}_2$  at  $450^\circ\text{C}$  for 2 h before preparing the cermets.  $\text{Cu}_2\text{O}$  and Cu powders were ball milled in dehydrated ethyl alcohol for 12 h. The powders were dried in a vacuum oven at  $80^\circ\text{C}$  after they were mixed.

After being dried, the mixed powders were hot pressed in a graphite die at  $1000^\circ\text{C}$ . The heating rate was  $20^\circ\text{C}/\text{min}$ . After the temperature reached  $1000^\circ\text{C}$ , the pressure was gradually increased to 25 MPa, and held for 40 min. The atmosphere in the hot pressing furnace was maintained at 1 atm of argon from the start to the end of the hot pressing procedure. The Cu contents ranged from 14.4 vol.% to 26.5 vol.% with 3.4 vol.% interval. The bulk density measurements show that the relative densities of the final cermets were all above 97%.

The thermal expansion was measured with a high temperature dilatometer (NETZSCH DIL 402C/3/G). The dimensions of the rectangular specimens were  $4\text{ mm} \times 4\text{ mm} \times 9\text{ mm}$ . The testing temperature was ramped from room temperature to  $900^\circ\text{C}$  with a ramp rate of  $5^\circ\text{C}/\text{min}$ . The test chamber was back-filled with 1.0 atm of argon from the start to the end of the thermal expansion test. In the present study, the CTE was calculated from the expansion data with the

following equation:

$$\alpha = \frac{\Delta L}{L_0} \frac{1}{\Delta T} \quad (3)$$

where  $\Delta L/L_0$  is the relative linear expansion and  $\Delta T$  is the temperature change.

### 3. Results and discussion

Fig. 2 shows the optical micrograph of the final cermets with Cu content of 26.5 vol.% prepared by branch-like and spherical Cu, respectively. It can be seen that the images are different and clearly show contrast arising from the ceramic phase and the metallic phase of the materials. The metallic phase, Cu, appears as light areas, while the ceramic phase,  $\text{Cu}_2\text{O}$ , appears as gray areas. The dark areas are the pores. Because the porosities of the final cermets are below 3%, it can be deduced that the dark areas are mostly pores resulted from the polishing process. It can be seen in Fig. 2a that the Cu phase is fiber like and randomly distributed. As demonstrated in Fig. 2b, the morphology of Cu phase is significantly different in Fig. 2a, most of them are round shape, and some of them are concentrated and formed agglomerates.

Fig. 3 shows the coefficients of thermal expansion (CTE) as a function of temperature of pure  $\text{Cu}_2\text{O}$  and Cu/ $\text{Cu}_2\text{O}$  cermets prepared by branch-like Cu and spherical Cu from room temperature to  $900^\circ\text{C}$ . Fig. 3a–d correspond to 14.4 vol.%, 18.3 vol.%, 22.3 vol.%, and 26.5 vol.% of Cu contents,

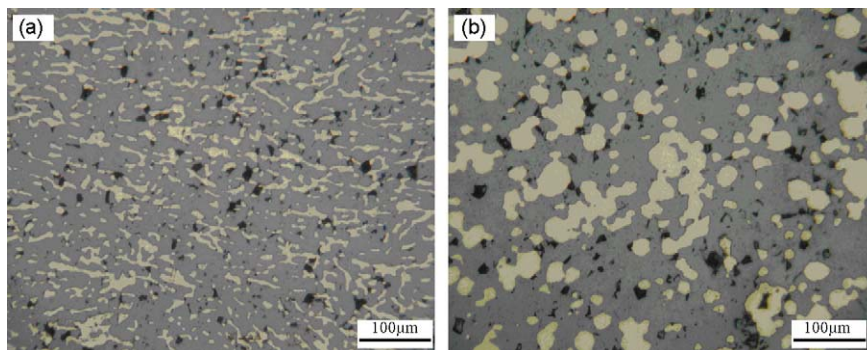


Fig. 2. Optical microstructures of the Cu/ $\text{Cu}_2\text{O}$  cermet with different Cu structures with (a) branch-like Cu and (b) spherical Cu.

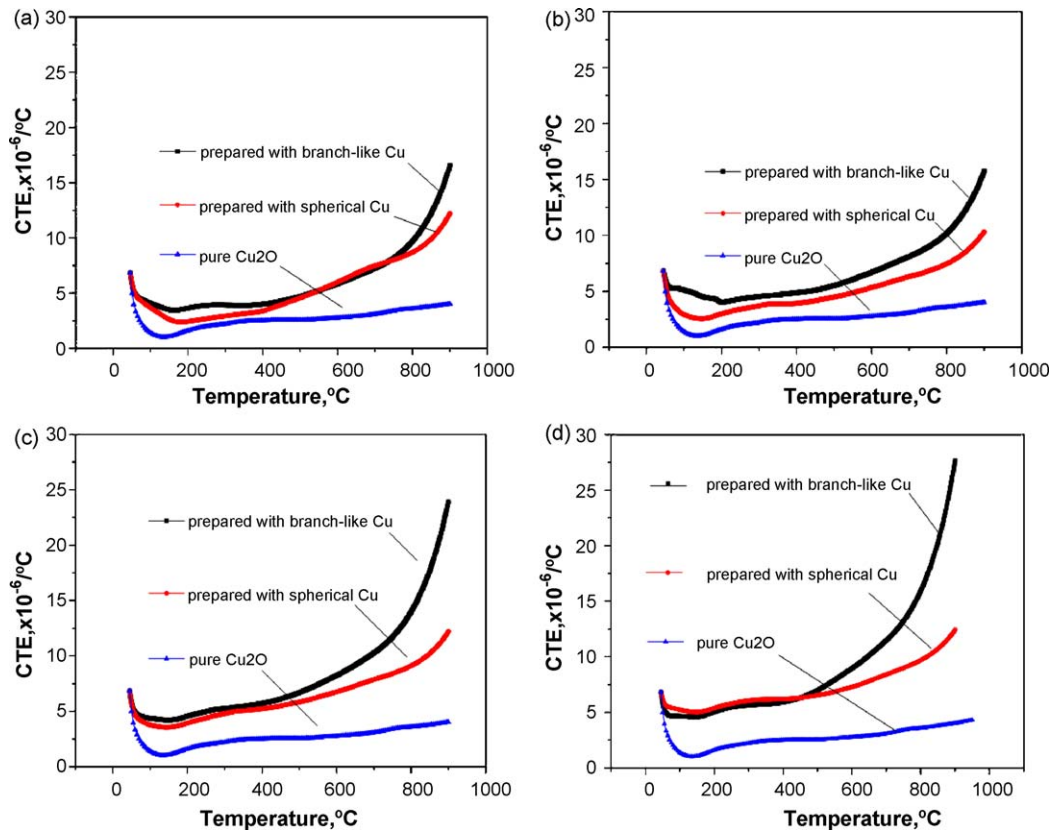


Fig. 3. CTE of pure  $\text{Cu}_2\text{O}$  and  $\text{Cu}/\text{Cu}_2\text{O}$  cermet prepared with branch-like and spherical Cu with (a) 14.4 vol.%, (b) 18.3 vol.%, (c) 22.3 vol.%, and (d) 26.5 vol.% of Cu content.

respectively. In this figure, the CTE curve, obtained from the  $\text{Cu}/\text{Cu}_2\text{O}$  cermets prepared with spherical Cu, can be separated into two segments. In the first segment, from room temperature to about  $150^\circ\text{C}$ , the slope of each curve is negative, demonstrating the CTE value decreases with increasing temperature, in the second segment, from  $150^\circ\text{C}$  to  $900^\circ\text{C}$ , the CTE linearly increases with increasing temperature. The CTE curves, which were obtained from cermets prepared with branch-like Cu, must be separated into three segments. In the first segments, from room temperature to about  $150^\circ\text{C}$ , the CTE values decrease with increasing temperature, similar to the behavior of the cermets with spherical Cu. In Fig. 3a and b, the second segments are from about  $150^\circ\text{C}$  to  $750^\circ\text{C}$ , and in Fig. 3c and d the second segments are from about  $150^\circ\text{C}$  to  $500^\circ\text{C}$ . In these segments, the CTE increasing rates with temperature are similar to those obtained from spherical Cu. However, in the third segments, from  $750^\circ\text{C}$  to  $900^\circ\text{C}$  in Fig. 3a and b, and from  $500^\circ\text{C}$  to  $900^\circ\text{C}$  in Fig. 3c and d, the CTE increasing rates with temperature are much higher than the second segments as well as those obtained from spherical Cu.

Through the comparison of the absolute CTE values, it is found that the CTE values increase with increasing Cu content in both  $\text{Cu}/\text{Cu}_2\text{O}$  cermets prepared with branch-like Cu and spherical Cu. In other studies, the CTE of a composite can be calculated with the rule of mixture. As reported previously [13], the CTE of pure  $\text{Cu}_2\text{O}$  increases linearly with increasing temperature from about  $2 \times 10^{-6}^\circ\text{C}^{-1}$  at  $150^\circ\text{C}$ , and  $3 \times 10^{-6}^\circ\text{C}^{-1}$  at  $900^\circ\text{C}$ . While in the same temperature

range, the CTE of pure Cu linearly increases with temperature from about  $16 \times 10^{-6}^\circ\text{C}^{-1}$  to  $25 \times 10^{-6}^\circ\text{C}^{-1}$  [14]. In this study, the CTE of the cermets prepared by spherical Cu was calculated with Eq. (1) from  $150^\circ\text{C}$  to  $900^\circ\text{C}$ . The calculation results were agreed well with experimental data. For the cermets prepared by branch-like Cu with 14.4 vol.% and 18.3 vol.% Cu, the theoretical CTE calculated by Eq. (1) agreed well in the temperature range from  $150^\circ\text{C}$  to  $750^\circ\text{C}$ , and those with 22.3 vol.% and 26.5 vol.% Cu in the temperature range from  $150^\circ\text{C}$  to  $500^\circ\text{C}$ , the CTE can be calculated based on this equation as well. However, for those prepared by branch-like Cu with 14.4 vol.% and 18.3 vol.% Cu in the temperature range from  $750^\circ\text{C}$  to  $900^\circ\text{C}$ , and those with 22.3 vol.% and 26.5 vol.% Cu in the temperature range from  $500^\circ\text{C}$  to  $900^\circ\text{C}$ , the experimental data of CTE did not agree with this equation. This discrepancy highlights the need of structural parameters in the model of CTE for  $\text{Cu}/\text{Cu}_2\text{O}$  cermet.

In a conductor–insulator composite, Balberg termed the second phase with two different structures [15,16]. According to his definition, the spherical shape has a “simplest structure” or “no structure”. The second phase in cermets with simple structure is distributed more regular than the one with complicated structure, because the connection probability of the particles with simple structure is lower than complicated structure, namely, different second phase structure will lead to different percolation channels and different connecting distributions. Thus, the conductivity properties based on percolation channels, mechanical properties based on cracks

propagation paths, or deformation behavior of the two phases will all be different. In the present study, the spherical Cu has a simpler shape than the branch-like Cu, therefore, the properties of those cermet with same volume fraction but with different second phase structures will not be the same.

In this study, the distribution of the branch-like Cu was a more random distribution of shapes in the spaces in between the  $\text{Cu}_2\text{O}$  matrix particles than those prepared with spherical Cu. In the high temperature range, extensive plastic deformation of  $\text{Cu}_2\text{O}$  can be observed [17], therefore, the CTE values of these two types are similar in the low temperature range because there were little plastic deformation of  $\text{Cu}_2\text{O}$  had occurred, however, there is a large difference in CTE at higher temperatures because the degree of plastic deformation of  $\text{Cu}_2\text{O}$  prepared with branch-like Cu is higher than those prepared with spherical Cu. In Cu/ $\text{Cu}_2\text{O}$  cermet, the deformation of  $\text{Cu}_2\text{O}$  is coming from the expansion of Cu due to its relatively high thermal expansion. For those Cu/ $\text{Cu}_2\text{O}$  cermets prepared with branch-like Cu, the quantity of percolation channels is higher than those prepared with spherical Cu. The more connected networks in these systems result in the higher strains on the  $\text{Cu}_2\text{O}$  matrix. In addition, the thermal stress behavior in real ceramics matrix composites with different shape of second phases was demonstrated by Hsueh's model [18]. The calculation results based on this model show that the thermal stress of the ceramic matrix composites increases with increasing aspect ratio of the second phase. Meanwhile, the

branch-like Cu leads to higher stress concentration than the spherical Cu, which results in higher thermal stress in the system, therefore, the CTE of Cu/ $\text{Cu}_2\text{O}$  cermets prepared with branch-like Cu is higher than those prepared with spherical Cu.

Fig. 4 shows the CTE as a function of temperature of prepared by branch-like Cu and spherical Cu from room temperature to 400 °C. Fig. 4a–d correspond to 14.4 vol.%, 18.3 vol.%, 22.3 vol.%, and 26.5 vol.% of Cu, respectively. This figure highlights the phenomenon of the decreasing rate CTE with increasing temperature of the first segments in Fig. 3. As shown in Fig. 4, the CTE curves of the cermets prepared with spherical Cu are similar and like a smooth “v” shape. The lowest value of CTE all occurred at about 150 °C for each content of Cu, which are 2.4, 2.6, 3.6, and 5.0 ( $\times 10^{-6} \text{ } ^\circ\text{C}^{-1}$ ) corresponding to 14.4 vol.%, 18.3 vol.%, 22.3 vol.%, and 26.5 vol.%, respectively. For those cermets prepared with branch-like Cu, the “v” shape is not as smooth as those curves obtained from the cermets prepared with spherical Cu, and the lowest values of CTE are 3.5, 4.1, 4.2, and 4.6 ( $\times 10^{-6} \text{ } ^\circ\text{C}^{-1}$ ) corresponding to 14.4 vol.%, 18.3 vol.%, 22.3 vol.%, and 26.5 vol.%, respectively. Both CTEs of cermets with low and high structural second phase are slightly increased with increasing Cu content.  $\text{Cu}_2\text{O}$  is a typical low thermal expansion material [19]. It was found that  $\text{Cu}_2\text{O}$  had a negative thermal expansion below  $-73 \text{ } ^\circ\text{C}$  (over the whole negative range is  $-2.4 \times 10^{-6} \text{ } ^\circ\text{C}^{-1}$ ) by X-ray powder diffraction [20] and subsequently it was found with a positive low coefficient of

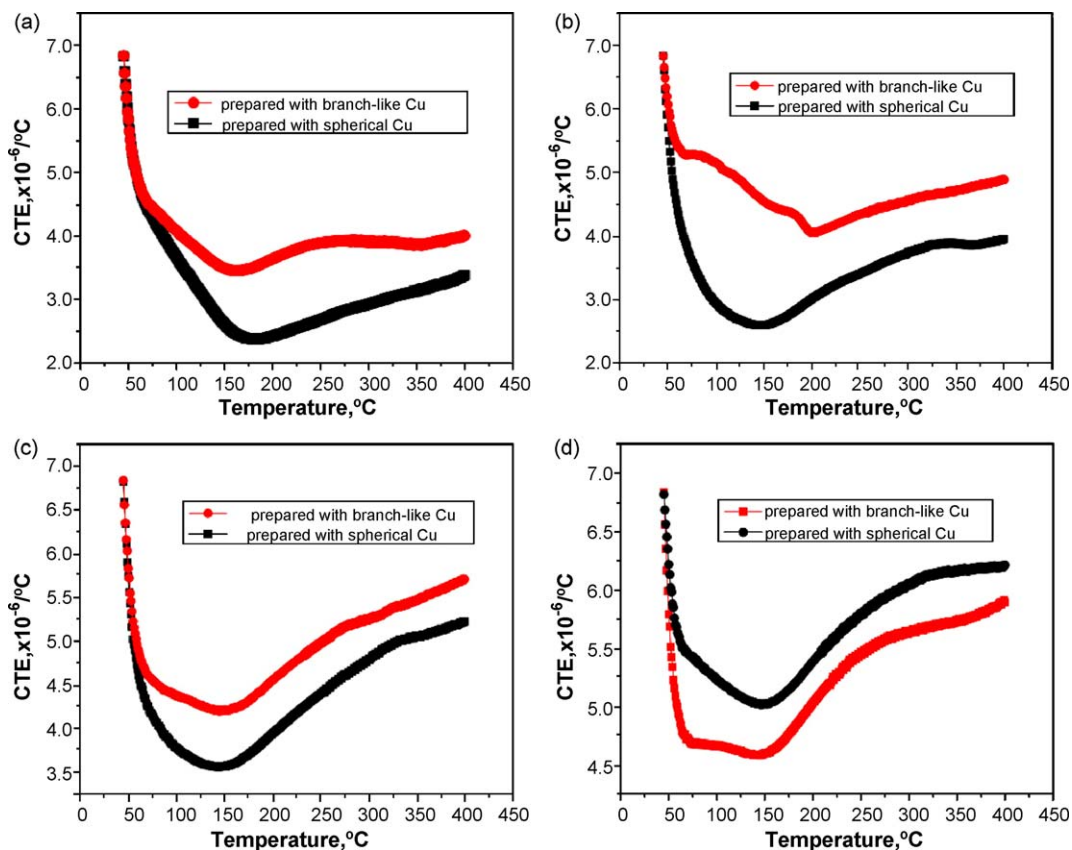


Fig. 4. CTE below 400 °C of Cu/ $\text{Cu}_2\text{O}$  cermet prepared with branch-like Cu and spherical Cu with (a) 14.4 vol.%, (b) 18.3 vol.%, (c) 22.3 vol.%, and (d) 26.5 vol.% of Cu content.



thermal expansion from 27 °C to 377 °C by neutron and synchrotron radiation X-ray diffraction [21,22]. In this temperature range, the anisotropic vibration of copper atoms is more intense in the plane perpendicular to the O–Cu–O bond than along this bond. This will lead to the lattice contraction of the Cu<sub>2</sub>O, and result in a decrease in the CTE. As shown in Fig. 4d, the lowest CTE value of the cermet prepared with spherical Cu is higher than the cermet prepared with branch-like Cu. This is different from Fig. 4a–c, in which the lowest CTE values prepared with spherical Cu are lower than the one prepared with branch-like Cu. In this case, the spherical Cu cannot form percolation channel until the weight fraction above 22.3 vol.%. Therefore, when the percolation channel was formed in the spherical Cu/Cu<sub>2</sub>O system, the heat is conducted along the percolation channel from the surface to the center quickly, then Cu phase in the center part is also heated quickly, making the whole sample expanded without obstruction from the Cu<sub>2</sub>O matrix, and therefore, the CTE value with 26.5 vol.% spherical Cu is higher than the one with 26.5 vol.% branch-like Cu in the low temperature range.

#### 4. Conclusions

In summary, Cu/Cu<sub>2</sub>O cermet with different Cu content were prepared with branch-like and spherical Cu powders. The results of CTE tests show that two types of CTEs both increase with increasing Cu content. In addition, these curves are not simply linearly increasing with temperature. For those cermet prepared by spherical Cu, the CTE curves are divided into two segments. The first segment is from room temperature to about 150 °C, in this segment, the CTE increasing rate decreases with increasing temperature; the second segment is from about 150 °C to 900 °C, in which the CTE increases linearly with increasing temperature. For those cermet prepared by branch-like Cu, however, the CTE curves are divided into three segments. The first segment is from room temperature to 150 °C, the CTE increasing rate decreases with increasing temperature as well, while the CTE increasing rate in the third segment is much higher than the second segment. For those with 14.4 vol.% and 18.3 vol.% of Cu, the second segment is from about 150 °C to about 750 °C, in this segment, the CTE increasing rate is similar to those derived from cermet prepared with spherical Cu, and the third segment is from 750 °C to 900 °C, the CTE increasing rate is higher than the second segment. For those with 22.3 vol.% and 26.5 vol.% of Cu, the second segment is from 150 °C to 500 °C, and the third segment is from 500 °C to 900 °C, namely, the CTE value of Cu/Cu<sub>2</sub>O cermet is not only a function of volume fraction of the second phase, but also a function of the structure of the second phase.

#### References

- [1] S.Y. Ahn, S. Kang, Effect of WC particle size on microstructure and rim composition in the Ti(C<sub>0.7</sub>N<sub>0.3</sub>)–WC–Ni system, *Scr. Mater.* 55 (2006) 1015–1018.
- [2] J. Johnson, J. Qu, Effective modulus and coefficient of thermal expansion of Ni–YSZ porous cermet, *J. Power Sources* 181 (2008) 85–92.
- [3] C.M. Grgicak, M.M. Pakulska, J.S. O'Brien, J.B. Giorgi, Synergistic effects of Ni<sub>1–x</sub>Co<sub>x</sub>–YSZ and Ni<sub>1–x</sub>Cu<sub>x</sub>–YSZ alloyed cermet SOFC anodes for oxidation of hydrogen and methane fuels containing H<sub>2</sub>S, *J. Power Sources* 183 (2008) 26–33.
- [4] R.P. Pawlek, Inert anodes: an update, *Light Metals* (2004) 283–287.
- [5] N. Xie, W.Z. Shao, L. Zhen, L.C. Feng, Electrical conductivity of inhomogeneous Cu<sub>2</sub>O–10CuAlO<sub>2</sub>–xCu cermet, *J. Am. Ceram. Soc.* 88 (2005) 2589–2593.
- [6] L.C. Feng, W.Z. Shao, L. Zhen, N. Xie, Microstructure and mechanical property of Cu<sub>2</sub>O–Cu cermet prepared by volume reduction-hot pressing method, *Mater. Lett.* 62 (2008) 3121–3123.
- [7] R. Saito, Y. Kondo, Y. Koike, K. Okamoto, T. Suzumura, T. Abe, Noble high thermal conductivity, low thermal expansion Cu–Cu<sub>2</sub>O composite base plate technology for power module application, in: *Proceedings of the 2001 International Symposium on Power Semiconductor Devices and ICs, Osaka, (2001)*, pp. 51–54.
- [8] X. Luo, Y. Yang, C. Liu, T. Xu, M. Yuan, B. Huang, The thermal expansion behavior of unidirectional SiC fiber-reinforced Cu-matrix composites, *Scr. Mater.* 58 (2008) 401–404.
- [9] A. Rudajevová, S. Kúdela, S. Kúdela, P. Lukáč, Anisotropy of the thermal expansion in Mg fibre composites, *Scr. Mater.* 53 (2005) 1417–1420.
- [10] O. Sigmund, S. Torquato, Composites with extremal thermal expansion coefficients, *Appl. Phys. Lett.* 69 (1996) 3203–3205.
- [11] Z.H. Karadeniz, D. Kumlutas, A numerical study on the coefficients of thermal expansion of fiber reinforced composite materials, *Compos. Struct.* 78 (2007) 1–10.
- [12] R.A. Schapery, Thermal expansion coefficients of composite materials based on energy principles, *J. Compos. Mater.* 2 (1968) 380–404.
- [13] L.C. Feng, W.Z. Shao, L. Zhen, N. Xie, V.V. Ivanov, Cu<sub>2</sub>O/Cu cermet as a candidate inert anode for Al production, *Int. J. Appl. Ceram. Technol.* 4 (2007) 453–462.
- [14] P. Abel, G. Bozzolo, Calculation of thermal expansion coefficients of pure elements and their alloys, *Scr. Mater.* 46 (2002) 557–562.
- [15] I. Balberg, A comprehensive picture of the electrical phenomena in carbon black-polymer composites, *Carbon* 40 (2002) 139–143.
- [16] I. Balberg, Tunneling and nonuniversal conductivity in composite materials, *Phys. Rev. Lett.* 59 (1987) 1305–1308.
- [17] G. Torres-Villasenor, R. Barrio-Paredes, S. Victor Radcliffe, The mechanical behaviour of cuprous oxide, *J. Mater. Sci.* 13 (1978) 2164–2170.
- [18] C.H. Hsueh, P.F. Becher, Residual thermal stresses in ceramic composites. Part I: with ellipsoidal inclusions, *Mater. Sci. Eng. A* 212 (1996) 22–28.
- [19] R. Roy, D.K. Agrawal, H.A. McKinstry, Very low thermal expansion coefficient materials, *Annu. Rev. Mater. Sci.* 19 (1989) 59–81.
- [20] M. Ivanda, D. Waasmaier, A. Endriss, J. Ihringer, A. Kirfel, W. Kiefer, Low-temperature anomalies of cuprite observed by Raman spectroscopy and X-ray powder diffraction, *J. Raman Spectrosc.* 28 (1997) 487–493.
- [21] W. Schafer, A. Kirfel, Neutron powder diffraction study of the thermal expansion of cuprite, *Appl. Phys. A: Mater. Sci. Process.* 74 (2002) S1010–S1012.
- [22] M. Dapiaggi, W. Tiano, G. Artioli, A. Sanson, P. Fornasini, The thermal behaviour of cuprite: an XRD-EXAFS combined approach, *Nucl. Instrum. Meth. B* 200 (2003) 231–236.